U.S.NRC
United States Nuclear Regulatory Commission
Protecting People and the Environment

Technical Letter Report
TLR-RES/DE/REB-2021-07
INL/EXT-21-62199

Benchmarking of Probabilistic Fracture Mechanics Models in Grizzly

Date:

Drafted: March 2021

Updated: June 2021

Published: September 2021

Idaho National Laboratory:

William M. Hoffman
Subject Matter Expert

Benjamin W. Spencer
Project Manager, Subject Matter Expert

NRC Project Manager:

Patrick Raynaud
Senior Materials Engineer
Component Integrity Branch

Division of Engineering
Office of Nuclear Regulatory Research
U.S. Nuclear Regulatory Commission
Washington, DC 20555–0001

DISCLAIMER

This report does not contain or imply legally binding requirements. Nor does this report establish or modify any regulatory guidance or positions of the U.S. Nuclear Regulatory Commission and is not binding on the Commission.

Executive Summary

In 2020, as part of contract/task order 31310019N0006/31310020F0060, the NRC tasked Idaho National Lab (INL) with benchmarking the MOOSE/GRIZZLY code against the NRC's Fracture Analysis of Vessels - Oak Ridge (FAVOR), version 16.1 code. Both codes can predict large light-water reactor vessel integrity deterministically and probabilistically. In fact, such predictions are the primary purpose of the FAVOR code, and are a main focus of the GRIZZLY code, although GRIZZLY is capable of modeling a wider range of geometries and problems. The vessel integrity modeling capabilities of the GRIZZLY code are still under development and being gradually expanded, and the capability to model vessel fracture by crack growth has not yet been integrated into GRIZZLY (although it does exist in pre-release versions). Thus, the present benchmark study focused on comparing predictions for the conditional probability of crack growth initiation (CPI) between GRIZZLY and FAVOR v16.1.

The present benchmarking study expands on a previous study completed in 2020, which focused on single plate regions, various flaw types, and full vessel studies. The previous study was limited in scope and revealed some relatively large discrepancies, particularly in the case of weld regions. In the present study, detailed investigations into the sources of discrepancies between GRIZZLY and FAVOR were performed, with a focus on weld regions.

The primary discrepancies identified were as follows:

- The weld fusion area was input differently in the two codes. Once corrected to ensure matching inputs, the differences between the codes were significantly reduced.
- The copper saturation content was computed differently in the two codes. Once a model matching the FAVOR v16.1 was implemented in GRIZZLY, the differences were significantly reduced.
- The distribution type for standard deviation of nickel can be either Weibull or Normal in FAVOR, and was initially set to Weibull, but GRIZZLY can only model Normal distributions. Once the distribution type was set to Normal in FAVOR, the differences were significantly reduced.
- The two codes have different methods to represent weld residual stresses through the vessel wall. Once GRIZZLY's model was modified to resemble FAVOR's more closely (although not exactly match it), the differences between the codes were reduced.

In all cases, once understood, the discrepancies were addressed in ways that significantly improved agreement between the two codes, such that the relative difference in predicted CPI between the codes was less than 5% in more than half of the benchmark cases, and less than 15% in all but one case. The largest CPI difference between the two codes was 72% relative, but only 1.21E-06 in absolute, which remains low. Overall, good agreement was achieved between GRIZZLY and FAVOR v16.1 for the range of problems studies.

Nonetheless some differences remained between the two codes, and could be the topic of future study if deemed necessary. These include: (1) the differences observed between the codes for embedded flaws, particularly in forging and weld regions; (2) differences in the way the codes treat surface-breaking flaws, especially infinite circumferential flaws; (3) differences in through-wall flaw distribution densities; and (4) the fact that GRIZZLY does not yet compute CPF, which would be an interesting quantity to study in future benchmarks.

INL/EXT-21-62199

Benchmarking of Probabilistic Fracture Mechanics Models in Grizzly

June 16, 2021

W. M. Hoffman and B. W. Spencer

Idaho National Laboratory
Idaho Falls, ID

INL/EXT-21-62199

Benchmarking of Probabilistic Fracture Mechanics Models in Grizzly

W. M. Hoffman and B. W. Spencer

Idaho National Laboratory
Idaho Falls, ID

June 16, 2021

Idaho National Laboratory
Idaho Falls, Idaho 83415

http://www.inl.gov

Prepared for the
U.S. Department of Energy
Office of Nuclear Energy
Under DOE Idaho Operations Office
Contract DE-AC07-05ID14517

Page intentionally left blank

Benchmarking of Probabilistic Fracture Mechanics Models in Grizzly

W. M. Hoffman and B. W. Spencer

Idaho National Laboratory
Idaho Falls, ID

June 16, 2021

1 Introduction

Under the U.S. Department of Energy's Light Water Reactor Sustainability (LWRS) and Nuclear Energy Advanced Modeling and Simulation (NEAMS) programs, the Grizzly code is being developed as a modern tool to address a variety of aging issues pertaining to the structural components of nuclear power plants. The original development focused on light-water reactors (LWRs), but more recent efforts were expanded to include issues pertinent to advanced reactors.

A major focus of LWR capability development in Grizzly has been a predictive capability for fracture in reactor pressure vessels (RPVs) during transient events. RPV integrity is a major concern when considering the long-term operation of existing reactors, since the steel from which they are constructed becomes increasingly brittle over time due to exposure to the reactor environment, which includes a combination of radiation and relatively high temperatures. Safety concerns that arise during transient events include rapid re-flooding, where elevated tensile stresses in conjunction with lower temperatures exist in the RPV's interior regions, which experience the highest embrittlement. Flaws present in the vessel wall due to the RPV manufacturing process could serve as initiation sites for fracture, and the susceptibility of the material to fracture increases with exposure time.

Because of the considerable uncertainty regarding the nature of the flaw population and the material properties, this problem should be considered probabilistically. Grizzly provides a probabilistic fracture mechanics (PFM) capability for evaluating the thermo-mechanical response of the RPV during a transient, then performs Monte Carlo (MC) simulations that evaluate large numbers of random realizations of the flaw population characteristics. In such MC analyses, the local stress conditions at specific flaw locations are utilized to evaluate mode-I stress intensity factors (K_I), which are, in turn, used together with the temperature and sampled local material properties (along with an embrittlement model) to compute the probability of crack initiation, given the occurrence of that particular transient.

These probabilities for individual flaws are used to compute a composite conditional probability of crack initiation (CPI) for the current realization of the flaw population. Because the CPI is generally quite low (values ranging from 1×10^{-7} to 1×10^{-3} are common), it can significantly vary from one RPV realization (MC iteration) to the next. The quantity that is ultimately of interest is the average CPI computed from all the MC iterations, which reaches a converged value after a sufficient number of iterations. The CPI is one of the key metrics of interest for such calculations. Another related quantity, the conditional probability of failure (CPF), indicates the probability of a crack propagating through the vessel given the occurrence of a transient. For a given transient, CPF is by definition less than or equal to CPI because for a crack to propagate through

the vessel wall, it must first initiate. The present effort is focused on CPI calculations because although a preliminary capability to compute CPF in Grizzly has been demonstrated, this capability has not yet been integrated into the main Grizzly code. More development effort is still needed to bring that capability to the point where it is ready for extensive testing of the nature performed here.

The process employed by Grizzly for PFM is based on the FAVOR code [3, 18]. Grizzly includes important additional features, including the ability to perform PFM analyses based on 1D, 2D, or 3D models of the RPV. This is important for capturing local variations in the internal surface conditions, as has been demonstrated on a local region in an RPV [12], as well as on a full RPV subjected to a postulated scenario that included prescribed temperatures to approximate the effects of a cold plume [14]. Grizzly's modular, flexible architecture readily permits switching to different models for various parts of the PFM simulation. This flexibility was demonstrated in the aforementioned 3D simulations, as well as in simulations that read neutron fluence maps directly from full-core neutronic simulations performed using VERAShift [15]. The fact that Grizzly can also perform PFM simulations in parallel greatly facilitates its usability, since these simulations can take multiple days on a single processor.

The PFM algorithm involves many complex steps, including finite element simulation of the RPV's global response, reading local results for specific flaws from that global model, using reduced-order models to compute K_I for individual flaws, randomly sampling material properties and flaw geometries, computing material embrittlement, computing the local CPI, and computing the average CPI from the MC iterations. To develop confidence in these recently developed Grizzly capabilities prior to using them on consequential applications, it is important to ensure that the algorithms were implemented correctly.

Testing of computational codes typically involves a combination of verification (comparison with known analytical solutions) and validation (comparison with experimental results). Whenever feasible, the algorithms used by Grizzly were verified against analytical solutions. For example, the core thermal and mechanics models provided by the MOOSE framework (upon which Grizzly is based) were verified against analytic solutions [9, 17]. Likewise, the capabilities for direct computation of fracture integrals were verified against analytic solutions [5, 11], as well.

The probabilistic RPV integrity problem does not lend itself well to validation, due to the extremely high cost of large-scale experiments and the low probability of failure. The models used to predict the shift in transition temperature [7] are based on an extensive experimental database of fracture tests, but it is challenging to validate this at the RPV scale where a fracture would initiate under given conditions.

Although not as rigorous as validation or verification, benchmarking with another code that implements the same algorithms remains a valuable exercise in terms of developing confidence in a predictive simulation tool. At a minimum, it ensures that the two codes being compared have implemented the same algorithms correctly. Because Grizzly largely uses the same algorithms for PFM calculations as FAVOR, it is natural to compare these two codes on problems that can be simulated using either code. Although Grizzly offers 3D capabilities, its PFM simulations in this study are based on global 1D models of the RPV response. These should provide results very similar to those from FAVOR, if implemented correctly.

2 Summary of Work Performed

Previous efforts have been made to benchmark Grizzly against FAVOR. Initial comparisons of a single plate region were included in [12], and a more recent study [13] compared Grizzly and FAVOR solutions for an expanded set of problems that included analyses of single regions with specific flaw types, as well as analyses of full RPVs that included assemblies of multiple region types such as plates and welds. That prior effort was somewhat limited in the set of options tested, and while agreement was quite good in many cases, some of the region types, particularly welds, showed discrepancies large enough to warrant further investigation.

The current effort builds on the referenced 2020 study, further improving Grizzly's RPV benchmarking

test suite. This includes a detailed investigation into the sources of the discrepancies between Grizzly and FAVOR, with a particular focus on weld regions. Details on the findings of this investigation are provided in Section 3. In addition, the Grizzly benchmarking test suite was expanded to include more options regarding the material types for plate and weld regions, as described in Section 4. Over the course of this benchmarking work, several areas of the PFM algorithm that were sources of confusion were encountered, and are now documented as lessons learned in Section 5. Although some of these issues are brought up throughout this report, individuals performing PFM analyses may find it helpful that each identified issue is listed in Section 5.

All the test cases studied here are part of the Grizzly assessment test suite, which consists of relatively large models run on a nightly or weekly basis (depending on the size of the problem. These are located in the `assessment/rpv_pfm/benchmark/1d` directory in the Grizzly source code repository. These cases all reference the same global model result for the transient loading, as provided in [13]. There are multiple subdirectories within that directory for the various cases, and each case includes the Grizzly input file, documentation of that case, reference solutions against which the current results are checked, and, because these particular tests are compared against FAVOR, the FAVOR input file and FAVOR solution file for reference. The corrections made to resolve discrepancies were applied to the versions of these test cases in the Grizzly repository, and the newly added cases were put in the Grizzly repository, as well. All results reported here reflect the current state of this test suite.

3 Identified Sources of Discrepancies

To investigate the discrepancies between the Grizzly and FAVOR solutions pertaining to the weld regions, parameter data from the randomly sampled flaw populations were output from both codes and then compared. A study of these data revealed issues in the following areas:

- **Weld fusion area**: Initial investigations into the discrepancy between the behavior of each code's weld model quickly revealed a difference in the FAVOR and Grizzly input files for these cases. The prescribed weld fusion areas specified in the FAVOR and Grizzly input files did not match each other. The weld fusion area is defined as the area of the weld that contacts the non-weld material. For circumferential welds, this is the cross-sectional area of the top and bottom of the subregion; for axial welds, it is the cross-sectional area of the sides of that subregion. Correcting the inconsistent inputs (for FAVOR, in this case) to the appropriate value and re-running the simulation significantly reduced the error between the two codes, though it remained larger than the errors of the the plate or forging models.

- **Cu saturation**: Before this benchmarking effort, the Grizzly implementation of the EONY embrittlement model was based on the description in [7]. Investigation of the differences of the two models revealed that the maximum effective Cu in solution (Cu_e) was computed differently in FAVOR than in Grizzly. Further research revealed three different published versions of the method for computing that value: one in Eason et al. (2006) [6], one published in the FAVOR theory manual [18], and one in Eason et al. (2013) [7]. Specific details on these models are provided in Section 5.2. Options were added to Grizzly so as to make all three of these versions available, and when the FAVOR 16 option is used in Grizzly, the computed CPI shows much better agreement between the codes.

- **Distribution types for standard deviation of Ni**: During the benchmarking efforts, another source of discrepancy between the two codes was found, specifically pertaining to weld models. FAVOR includes an option for specifying the distribution type (i.e., normal or Weibull) for sampling of the standard deviation for nickel content in welds. On the other hand, the only option currently provided

by Grizzly is to use a normal distribution. The benchmark models were constructed in FAVOR to use Weibull distributions, resulting in some variation between the codes. The FAVOR models were modified to use the normal distributions in order to match Grizzly, then re-run. The option to use a Weibull distribution still needs to be added to Grizzly.

- **Method for Defining Residual Stresses**: FAVOR allows for the effects of residual stresses to be accounted for in weld regions by computing K_I due to the residual stresses and adding that to the value of K_I caused by the transient loading. An initial approach to account for residual stresses in a similar way had been previously implemented in Grizzly. That approach read the polynomial coefficients for a fit to the through-wall residual stress profile from a user-provided file. However, because of the nature of the stress profile, it is not represented well by a single low-order fit all the way through the wall, so the Grizzly results did not match FAVOR's very well in some cases. A newer model in Grizzly for residual stresses that better matches the behavior of FAVOR was used in the current work, and provides better agreement with FAVOR solutions. More details on the residual stress computation procedure are provided in Section 5.7.

4 Expanded Set of Test Cases

In addition to resolving discrepancies between the existing models, the benchmarking test suite was expanded to include additional options to more fully test the code. The additions to the test suite are summarized as follows:

- New weld models: Previous benchmark efforts only included testing of one weld type (`OTHER`) within Grizzly. Furthermore, models for only two weld types were implemented in the code at that time. Based on the findings of the current work, Grizzly was expanded to support three weld types:
  - LINDE_80 – Linde 80 weld weld types
  - LINDE_1092 – Linde 1092 weld types
  - OTHER – all other weld types

  All three of these weld types are tested nightly via our automatically run test suite, both with and without the effects of residual stress for the weld only models.
- New plate model: The early PFM benchmarking of plate regions in Grizzly included Combustion Engineering (CE) plates only. Cases for non-CE plates have also been added for all flaw types.

5 Lessons Learned

Over the course of both the current benchmarking exercise as well as prior efforts, multiple issues were encountered that resulted in discrepancies between Grizzly and FAVOR. Some of these reflected problems with the algorithms, while some simply involved instances in which the code behavior was not readily apparent. Since these issues could potentially be of concern to someone running either code, they are documented here in hopes of helping others undertake similar exercises in the future.

5.1 Sampling Embedded Flaw Depths with Cladding

In the initial benchmarking of Grizzly on a single plate region (as documented in [12]), histograms of all of the sampled variables were generated for both Grizzly and FAVOR in order to ensure that the generated samples matched with a sufficiently high number of MC iterations. This exercise revealed a discrepancy

between the codes in terms of the sampled depths of embedded flaws, as shown in Figure 1a. Both codes show a decreased number of samples near the inner wetted surface. This is expected because the embedded flaws only occur in the base metal, meaning that there are no flaws in the cladding.

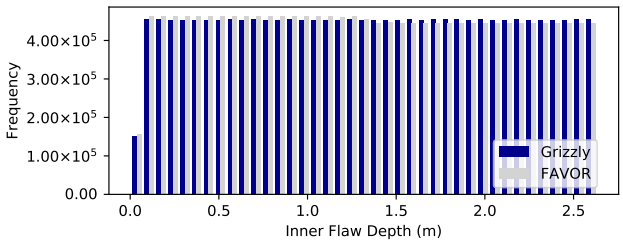

(a) Flaw depth distribution before correction to FAVOR

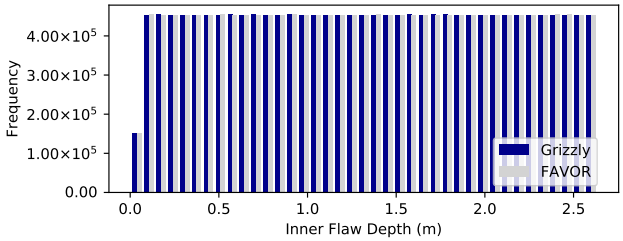

(b) Flaw depth distribution after correction to FAVOR

Figure 1: Histogram of flaw depths sampled using Grizzly and FAVOR for a single plate region, before and after correction to FAVOR.

The flaws should be uniformly distributed across the full base-metal region, but FAVOR shows a slightly higher concentration of flaws on the inner half of the vessel, and a slightly lower concentration on the outer half. This behavior disappears when there is no cladding. This was found to be caused by the fact that FAVOR independently distributes the flaws over the inner and outer halves of the vessel, but uses the midpoint of the entire wall rather than the midpoint of the base metal in this process. For cooldown transients, which are controlled primarily by flaws on the inner half of the vessel, this results in slightly conservative solutions.

Since this is not believed to be the desired behavior, a modified version of FAVOR 16.1 that corrects for this issue was used to provide the FAVOR solutions in the present exercise. Figure 1b shows that the Grizzly and FAVOR flaw distributions match up very well with this correction.

5.2 Multiple Methods for Computing Cu Saturation

The EONY model used for both the Grizzly and FAVOR solutions in this exercise has an upper bound on the effective Cu in solution (Cu_e). If the sampled wt. % of Cu for a given flaw exceeds this limit, it is set to the limiting value. The initial implementation of the EONY model in Grizzly was based on [7]. Discrepancies in the computed CPI values between Grizzly and FAVOR were found to originate in differences regarding how the maximum Cu_e is computed in different variants of this model. The 2006 report [6] computes this slightly differently than the 2013 paper; in turn, the version of the model documented in the FAVOR 16.1 manual [18] and known as "Eason 2006" also differs slightly from both these versions. Apart from this maximum Cu_e, no other differences among these versions of the model were identified.

The maximum amount of copper available for precipitation is dependent on the weld type and nickel (Ni) concentration in that particular subregion. The logic for determining the maximum Cu_e is summarized here for each of the three model variants. For the FAVOR 16.1 implementation of the Eason 2006 model, it is

computed as:

$$\max(\mathrm{Cu_e}) = \begin{cases} 0.301 & \text{for Linde 1092 welds} \\ 0.2435 & \text{for Linde 80 or Linde 1092 welds where (0.5wt\% < Ni < 0.75 wt\%)} \\ 0.370 & \text{for Linde 80 or Linde 1092 welds where Ni < 0.5wt\%} \\ 0.301 & \text{for all other materials} \end{cases} \tag{1}$$

In the Eason et al. 2006 report, it is computed as:

$$\max(\mathrm{Cu_e}) = \begin{cases} 0.243 & \text{for typical (Ni > 0.5 wt\%) Linde 80 welds} \\ 0.301 & \text{for Linde 1092 welds} \\ 0.370 & \text{for all other materials} \end{cases} \tag{2}$$

Finally, in the Eason et al. 2013 paper, it is computed as:

$$\max(\mathrm{Cu_e}) = \begin{cases} 0.243 & \text{for typical (Ni > 0.5 wt\%) Linde 80 welds} \\ 0.301 & \text{for all other materials} \end{cases} \tag{3}$$

To facilitate benchmarking against FAVOR and clarify to the user which variant of the model is being used, a required parameter was added to the Grizzly input file in order to specify the model version. The options for this parameter are:

- `FAVOR16_EASON_2006`: Replicates the "Eason 2006" model in the FAVOR 16.1 code, which differs slightly from the Eason et al. 2006 report
- `EASON_2006`: Exactly as described in the Eason et al. 2006 report
- `EASON_2013`: Exactly as described in the Eason et al. 2013 paper.

In addition, Grizzly did not originally provide options for multiple weld types, but users must now specify one of the following three options to define the weld type:

- `LINDE_80`: Linde 80 weld weld types
- `LINDE_1092`: Linde 1092 weld weld types
- `OTHER`: All other weld types.

5.3 Switching between Reduced-Order Fracture Models for Surface-Breaking Flaws

Historically, FAVOR utilized direct fracture mechanics simulations to compute stress intensity factor influence coefficients (SIFICs) used to calculate K_I for surface-breaking flaws. However, recent versions of Section XI, Appendix A-3000, of the ASME Boiler and Pressure Vessel Code provide solutions for a variety of flaw geometries [1]. Starting in 2017, these have been provided for both axial and circumferential surface-breaking flaws, and Grizzly directly utilizes these solutions for all surface-breaking flaws. The SIFICs provided by the ASME code are applicable to flaws in the base metal, and the ASME code does not provide SIFICs for the contributions of cladding stresses to K_I. The cladding effects are superimposed on the base-metal response, and both Grizzly and FAVOR account for the cladding using interpolations from a set of SIFICs for the cladding that was developed for FAVOR using finite element simulations.

For the base metal, FAVOR 16.1 uses the SIFICs from the ASME code, but, for various reasons, switches between the models in some cases. For axial flaws, it always uses the A-3000 SIFICs. For finite circumferential flaws, however, it uses the standard A-3000 circumferential SIFICs when the ratio of flaw depth (a) to vessel thickness (t), a/t, is less than 0.5. For a/t=0.5, it uses the A-3000 axial SIFICs. For finite surface-breaking flaws, FAVOR computes K_I at a set of 8 discrete flaw depths with a maximum depth of 0.5 and interpolates between them, so this switching between models has some effect on flaws with a/t less than, but approaching 0.5. For infinite flaws, it uses the standard A-3000 circumferential flaw models if the a/t is less than 0.2, but uses the models based on fracture mechanics solutions used in older (pre-2015) versions of FAVOR if a/t is greater than 0.2.

To facilitate benchmarking against FAVOR 16.1, an option to mimic its methodology of switching between models was made available in Grizzly, and is used in the present work. However, this model currently does not completely replicate FAVOR 16.1's behavior, since Grizzly does not currently have the pre-2015 FAVOR SIFICs implemented. Thus, for infinite circumferential flaws, some variation between the codes will remain, even with this compatibility option enabled.

5.4 Handling of Scenarios Involving Fractional Flaw Sampling

The algorithm used by FAVOR to generate the flaw population in an RPV generates a real number for the total number of flaws, based on the specified flaw density. The actual number of flaws generated in a given RPV is that number rounded down to the nearest integer. This same behavior is implemented in Grizzly. If there is a large number of flaws, this does not have a major effect; but if there is a small number of flaws, as is often the case with surface-breaking flaws, this can be a significant source of error. The earlier benchmarking exercises documented in [14] had some surface-breaking flaw cases that indicated that CPI = 0. This was because the number of flaws for the region being investigated was slightly less than 1, so no flaws were generated. The current study increased these areas by a factor of 2 so as to always generate at least one flaw.

A recommended enhancement to both codes is to carry the non-integer remainder through to the next RPV realization, so that, on average, the desired flaw density will be generated.

5.5 Output Quantities for Transition Temperature Shift

The embrittlement models in FAVOR automatically apply scaling factors of 1.1 and 0.99 (for welds and other regions, respectively) to the computed transition temperature shift. This is done for all PFM calculations, but not when output is requested. The reasons for this were not immediately clear in this investigation, initially leading to some confusion when comparing results.

Further investigation clarified that the embrittlement models compute the change in the transition temperature for the Charpy V-notch toughness (ΔT_{30}). The 1.1 and 0.99 factors come from correlations that define the relationship between ΔT_{30} and the change in the reference nil-ductility temperature, ΔRT_{NDT}, which is the quantity used in RPV fracture evaluations. These correlations are defined in Section 4.2.3.3 and Figure 4–39 of [8].

5.6 Prescribed Weld Fusion Area

In both FAVOR and Grizzly, the weld fusion area is required as an input parameter. There is no obvious reason for this, since it can be directly computed from the other required input parameters i.e., wall thickness, angular extent, height, orientation. Discrepancies in the results were encountered on multiple occasions when the weld fusion area was not specified in a manner consistent with the other parameters for that region. For both codes, an investigation should be made into whether this parameter can be computed within the code, thus ensuring that it will be correctly computed for every simulation, leaving less opportunity for user error.

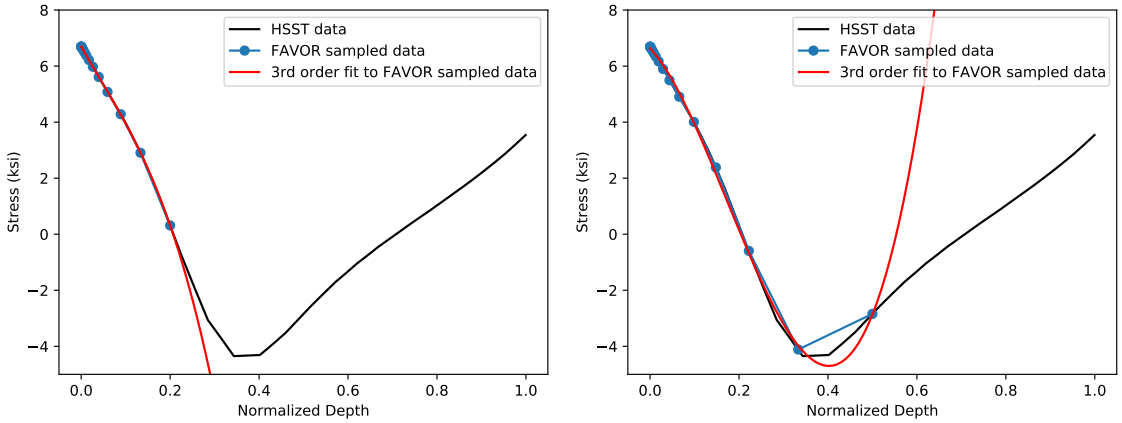

Figure 2: Through-wall variation of residual stress from the HSST program as sampled by FAVOR and fit with a 3rd order polynomial using those sampling points for a finite surface-breaking flaw with a normalized depth of 0.2 (left), and a finite surface-breaking flaw with a normalized depth of 0.5 (right)

5.7 Treatment of Residual Stresses

FAVOR applies a stress profile was developed based on experimental measurements of an axial weld in a reactor pressure vessel (RPV). This was based on data from a canceled plant taken by the Oak Ridge National Laboratory (ORNL) Heavy Section Steel Technology (HSST) program, as documented in [10] and [2]. Finite element simulations were performed [4] to infer the through-wall distribution of the residual stresses.

This through-wall residual stress profile has a shape that is not fit well by the relatively low order polynomials typically used in the weight-function approach for computing K_I. In a prior effort to provide these HSST residual stresses in Grizzly [16], it was found that while lower (3rd or 4th) order polynomials can provide a reasonable fit for certain regions of the vessel wall, an 8th order polynomial is required to fit this profile across the entire wall. This presents a challenge because the SIFICs provided by the ASME Boiler and Pressure Vessel Code only support up to a 4th order polynomial representation of the stress profile.

FAVOR uses 3rd order polynomials for surface-breaking flaws, and performs least-squares fitting of a set of data points sampled from the through-wall stress distribution to compute the coefficients of the polynomials for a discrete set of flaw depths. It then uses those coefficients to compute K_I at those depths, and interpolates between those computed K_I values for other flaw depths.

Attempting to better match the FAVOR behavior led to an in-depth investigation of how these polynomial coefficients are computed by FAVOR, and it was found that the results are affected significantly by the choice of points where the stresses are sampled for use in the least-squares fitting to compute the coefficients. Figure 2 shows the baseline HSST residual stress data, along with the discrete points sampled from the stress profile and the resulting 3rd order polynomial that is computed from those points using least-squares fitting for two different depths. FAVOR computes the total stresses as a summation of the stresses induced by the transient loading and the residual stresses, uses a cubic spline procedure to smooth those stresses, and then samples that smoothed data at the discrete points indicated in that figure. As is evident in that figure, the sampling points are concentrated near the inner wetted surface, where the gradients are typically largest. However, in cases with deep flaws where the residual stresses are significant, there are very few points near the tip of the flaw, where the stress gradients can also be quite large. For shallower flaws (with a flaw depth to wall thickness ratio less than about 0.2), the fitted polynomial reasonably matches the residual stress profile over the flaw, but for deeper flaws, the agreement between the fitted polynomial and the residual stress profile is quite poor, especially in terms of their gradients at the crack tip.

Table 1: Comparison of the final CPI values for FAVOR and Grizzly, both before (left) and after (right) this benchmarking effort. Cases with residual stresses included are denoted as "RS." All other cases do not include residual stresses. Cells colored in red have a relative difference greater than 20%, those colored in yellow have a relative difference between 5% and 20%, and those colored in green have a relative difference less than 5%.

Old Results				
Embedded Only	Grizzly CPI	FAVOR CPI	Error %	RPV Realizations
Plate	9.24E-07	1.07E-06	13.4	1M
Forging	2.09E-07	2.29E-07	8.7	1M
Weld	2.53E-05	3.82E-05	33.6	500k
Weld RS	1.70E-04	1.79E-04	5.1	500k
Plates and Welds	5.82E-05	6.03E-05	3.6	200k
Forgings and Weld	2.92E-06	1.64E-06	77.7	500k
Surface Breaking Only				
Plate	1.18E-03	1.18E-03	0.1	1M
Forging	6.41E-04	6.53E-04	1.7	1M
Weld	0.00E+00	0.00E+00	0.0	1M
Weld RS	0.00E+00	0.00E+00	0.0	1M
Plates and Welds	9.63E-02	9.69E-02	0.7	100k
Forgings and Weld	9.27E-03	1.01E-02	8.3	500k
Embedded and Surface Breaking				
Plate	1.76E-03	1.76E-03	0.0	1M
Forging	7.28E-04	7.38E-04	1.5	1M
Weld	2.52E-05	3.28E-05	23.1	1M
Plates and Welds	9.73E-02	9.70E-02	0.4	10k
Forgings and Weld	9.36E-03	1.03E-02	8.8	100k

New Results				
Embedded Only	Grizzly CPI	FAVOR CPI	Error %	RPV Realizations
Plate CE	9.24E-07	9.77E-07	5.4	1M
Plate Non-CE	2.16E-07	2.27E-07	5.0	1M
Forging	2.09E-07	2.29E-07	8.7	1M
Weld Other	2.96E-05	3.16E-05	6.2	500k
Weld Other - RS	1.71E-04	1.98E-04	13.8	500k
Weld L80	2.96E-05	3.16E-05	6.2	500k
Weld L80 - RS	1.71E-04	1.98E-04	13.8	500k
Weld L1092	2.53E-05	2.71E-05	6.5	500k
Weld L1092 - RS	1.47E-04	1.70E-04	13.7	500k
Plates and Welds	5.81E-05	6.12E-05	5.1	400k
Forgings and Weld	2.89E-06	1.68E-06	72.1	400k
Surface Breaking Only				
Plate CE	1.18E-03	1.18E-03	0.1	1M
Plate Non-CE	3.73E-04	3.71E-04	0.4	1M
Forging	6.41E-04	6.53E-04	1.7	1M
Weld Other	8.05E-05	7.71E-05	4.4	1M
Weld Other - RS	3.16E-04	3.20E-04	1.2	1M
Weld L80	8.05E-05	7.71E-05	4.4	1M
Weld L80 - RS	3.16E-04	3.20E-04	1.2	1M
Weld L1092	7.11E-05	6.85E-05	3.9	1M
Weld L1092 - RS	2.85E-04	2.89E-04	1.2	1M
Plates and Welds	9.64E-02	9.67E-02	0.3	400k
Forgings and Weld	9.27E-03	1.01E-02	8.3	500k
Embedded and Surface Breaking				
Plate CE	1.76E-03	1.76E-03	0.0	1M
Plate Non-CE	5.54E-04	5.55E-04	0.2	1M
Forging	7.28E-04	7.38E-04	1.5	1M
Weld Other	2.96E-05	3.10E-05	4.4	1M
Weld L80	2.96E-05	3.10E-05	4.4	500k
Weld L1092	2.53E-05	2.63E-05	3.7	500k
Plates and Welds	9.74E-02	9.79E-02	0.5	400k
Forgings and Weld	9.37E-03	1.02E-02	8.4	400k

One of the major objectives of the present exercise is to establish that Grizzly has the basic PFM algorithm implemented correctly. A set of models that is common to both codes is necessary for a code-to-code comparison, so the residual stress calculation in Grizzly has been implemented to match FAVOR's behavior as closely as possible, despite this issue. Polynomials could be fit to better match the HSST data for deeper flaws by using sampling points that are more uniformly spaced through the depth of the flaw, and implementing a model that uses improved polynomial coefficients obtained in this manner is planned for future development.

6 PFM Benchmarking Results

The present effort served to significantly improve the agreement between FAVOR and Grizzly. As described in the previous sections, during the course of the present benchmarking effort, multiple sources of discrepancies between the two codes were resolved, reducing the variation in the codes' results. Table 1 summarizes the average CPI values for each case in the test suite, both before and after this study. This table highlights that the discrepancies between the codes were significantly reduced for the weld cases, and shows the extent to which the test suite was expanded.

After the efforts performed here, nearly all of the cases with only surface-breaking flaws or a combination of embedded and surface-breaking flaws show close agreement, with less than a 5% difference between the codes. The discrepancies are still somewhat higher for the cases with only embedded flaws, and in the case

of the model with forgings and welds, the discrepancy is still quite large (about 72% relative difference). These cases will still require further investigation to find the sources of these differences.

CPI convergence histories over the course of the MC iterations are shown for each individual case in the test suite. Figure 3 shows these histories for the plate models, Figure 4 shows them for the weld models with embedded flaws, Figure 5 shows them for the weld models with surface-breaking flaws, Figure 6 shows them for welds and forgings, and Figure 7 shows them for plates, welds, and forgings. There is a wide variety of final CPI values for these various cases. And as expected, cases with a higher CPI require fewer MC iterations to obtain a converged solution.

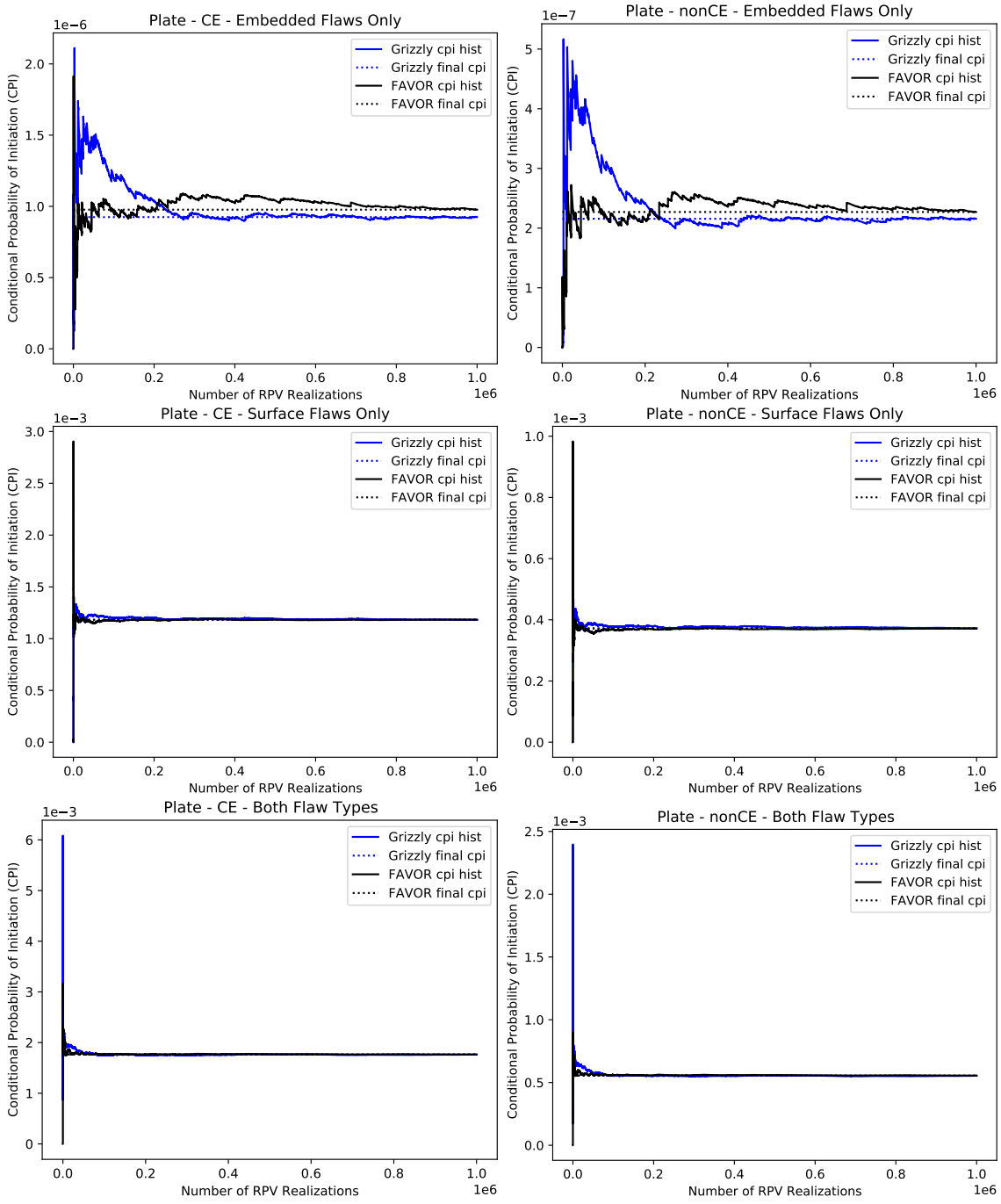

Figure 3: CPI convergence history for PFM plate models.

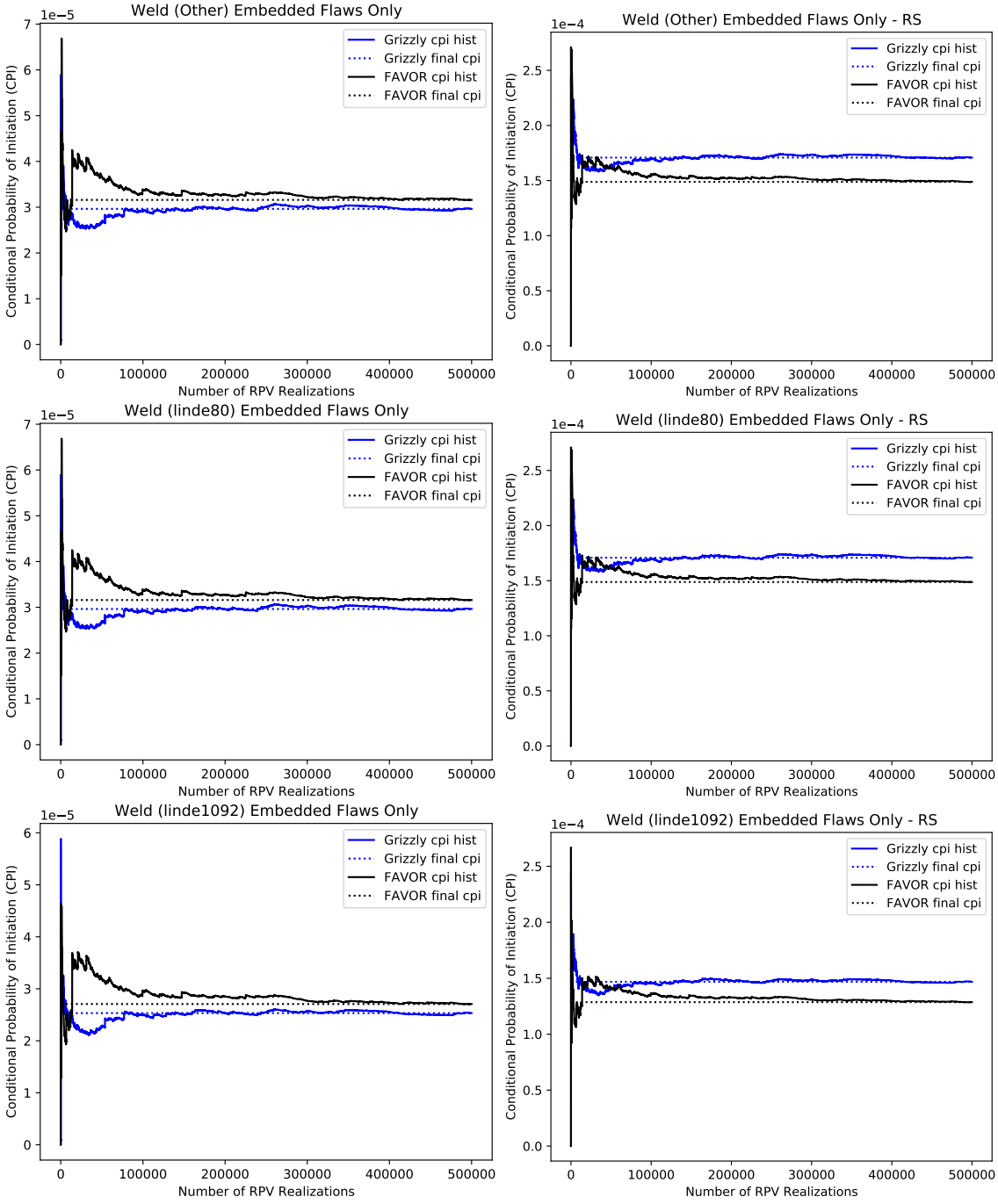

Figure 4: CPI convergence history for PFM weld models with embedded flaws.

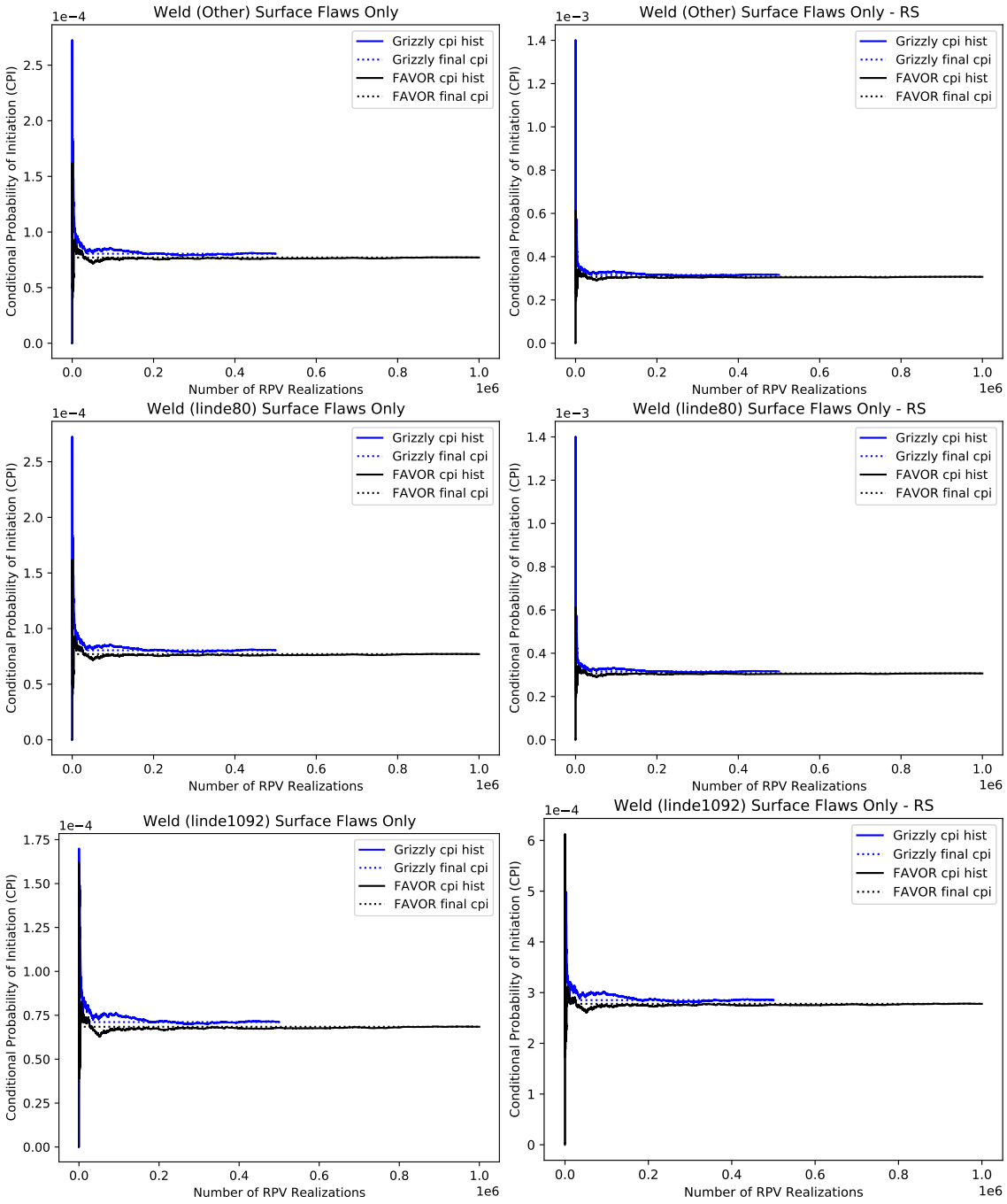

Figure 5: CPI convergence history for PFM weld models with surface breaking flaws.

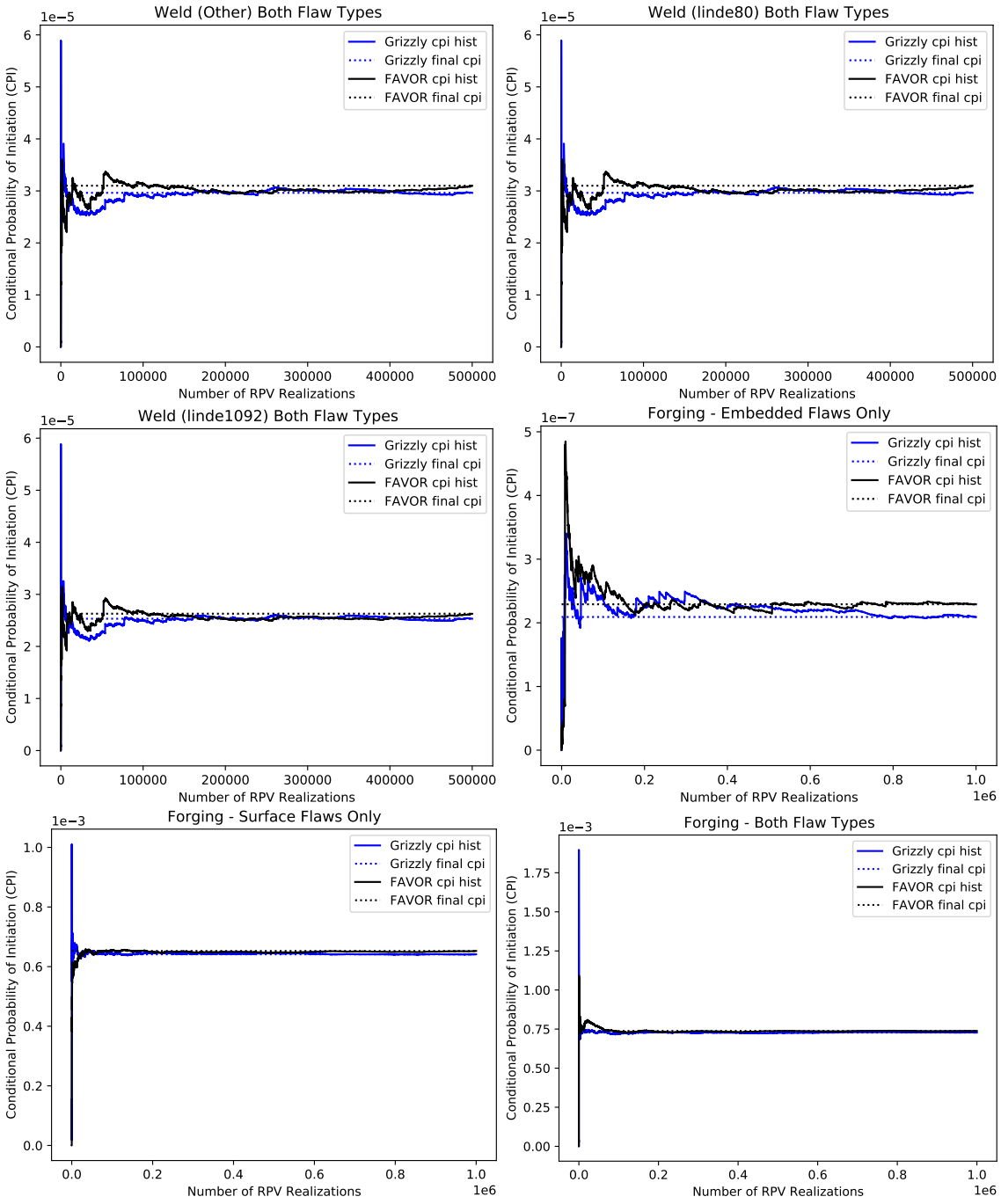

Figure 6: CPI convergence history for PFM weld and forging models.

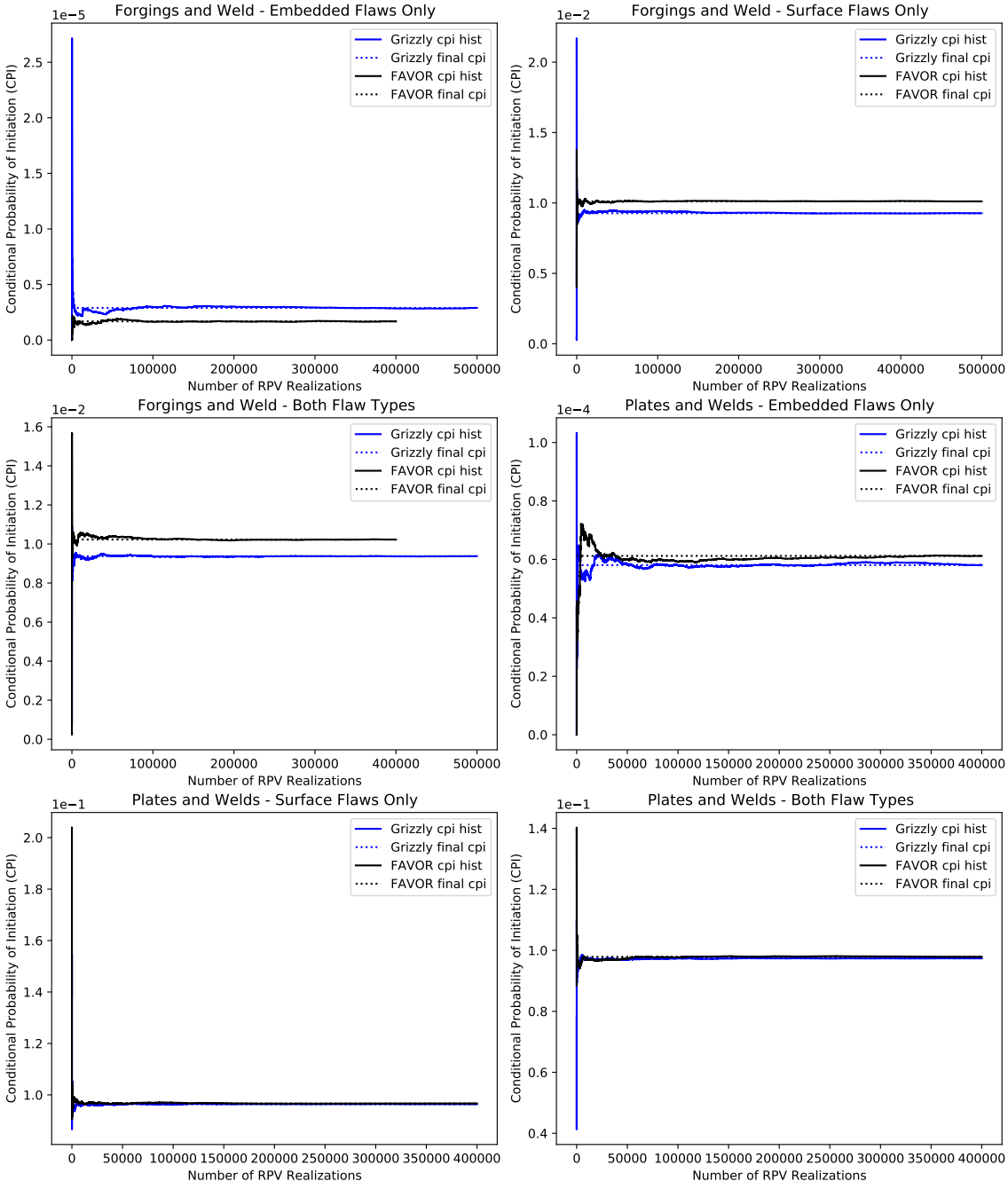

Figure 7: CPI convergence history for PFM plates-and-welds and forgings-and-weld models.

7 Summary

As detailed in this report, multiple issues regarding the weld problems in the Grizzly benchmarking test suite were resolved in order to minimize the differences between the Grizzly-obtained solutions and the reference FAVOR solutions. These issues included discrepancies in the model inputs for the two codes and subtle differences in the implementation of the algorithms. In resolving these issues, for most cases, the two codes' solutions for CPI were brought into reasonably close agreement. The test suite was also expanded to include a wider range of options, and the two codes' solutions for these newly introduced problems were generally in good agreement here, as well.

The following areas for further investigation or development could address some of the remaining discrepancies and test other aspects of these codes:

- The differences between the codes are largest for cases with only embedded flaws, especially for the model with forgings and welds. These cases still need further investigation.
- The Grizzly implementation of the FAVOR 16.1 compatibility option for surface-breaking flaws does not completely replicate the FAVOR behavior. Implementation of the FAVOR SIFICs for infinite circumferential flaws would be required for full compatibility.
- To match an unmodified version of FAVOR 16.1, Grizzly would require a compatibility option to generate the through-wall flaw depth distribution in the same way as FAVOR.
- The present study focused on computation of CPI, but CPF is also an important quantity that should be benchmarked using this same set of problems once the Grizzly implementation of the CPF calculation is sufficiently mature.

It is important to note that this benchmarking exercise benefits both Grizzly and FAVOR. The Grizzly PFM algorithms were based primarily on their descriptions in the FAVOR theory manual. By resolving observed discrepancies between the codes, this exercise identified issues with both codes, building confidence that both codes correctly implemented the documented algorithms.

Finally, this exercise establishes that Grizzly, with options set to facilitate FAVOR compatibility in certain areas of the algorithm, produces solutions that reasonably match those of FAVOR. However, development is underway to further improve on some of the algorithms. In particular, the reduced-order models for embedded flaw calculations are being updated in Grizzly to provide more accurate solutions and, in some cases, remove significant conservatisms. These benchmark problems will be used to quantify the effect of these changes on the computed CPI for a variety of cases. They also instill confidence that Grizzly's basic capabilities are correctly implemented, thus providing a solid foundation for applications that exercise Grizzly's capabilities for 3D analysis and coupling with neutronic simulations.

References

[1] American Society of Mechanical Engineers (2017). *ASME Boiler and Pressure Vessel Code, Section XI, Rules for Inservice Inspection of Nuclear Power Plant Components, Nonmanditory Appendix A, Article A-3000 Method of K_I Determination*. Number ASME BPVC.XI-2017.

[2] Corwin, W. R. (1988). Heavy-Section Steel Technology Program semiannual progress report for April–September 1988. Technical Report NUREG/CR-4219, ORNL/TM-9593 Vol. 5, No. 2, Oak Ridge National Laboratory.

[3] Dickson, T., Williams, P. T., Bass, B. R., and Klasky, H. B. (2016). Fracture Analysis of Vessels – Oak Ridge, FAVOR, v16.1, computer code: User's guide. Technical Report ORNL/LTR-2016/310, Oak Ridge National Laboratory, Oak Ridge, TN.

[4] Dickson, T. L., Bass, B. R., and McAfee, W. J. (1998). The inclusion of weld residual stress in fracture margin assessments of embrittled nuclear reactor pressure vessels. In *ASME Pressure Vessels and Piping Conference*, volume PVP-Vol. 373, Fatigue Fracture, and Residual Stresses.

[5] Dolbow, J., Zhang, Z., Spencer, B., and Jiang, W. (2015). Fracture capabilities in Grizzly with the eXtended Finite Element Method (X-FEM). Technical Report INL/EXT-15-36752, Idaho National Laboratory, Idaho Falls, ID.

[6] Eason, E., Odette, G., Nanstad, R., and Yamamoto, T. (2006). A physically based correlation of irradiation-induced transition temperature shifts for RPV steels. Technical Report ORNL/TM-2006/530, Oak Ridge National Laboratory.

[7] Eason, E., Odette, G., Nanstad, R., and Yamamoto, T. (2013). A physically-based correlation of irradiation-induced transition temperature shifts for RPV steels. *Journal of Nuclear Materials*, 433(1-3):240–254.

[8] EricksonKirk, M., Bass, B. R., Dickson, T., Pugh, C., Santos, T., and Williams, P. (2007). Probabilistic fracture mechanics – models, parameters, and uncertainty treatment used in FAVOR version 04.1. Technical Report NUREG-1807, U.S. Nuclear Regulatory Commission.

[9] Hales, J., Novascone, S., Spencer, B., Williamson, R., Pastore, G., and Perez, D. (2014). Verification of the BISON fuel performance code. *Annals of Nuclear Energy*, 71:81–90.

[10] Keeney, J., Bass, B., McAfee, W., and Iskander, S. (1994). Preliminary assessment of the fracture behavior of weld material in full-thickness clad beams. Technical Report NUREG/CR-6228, ORNL/TM-12735, Oak Ridge National Laboratory.

[11] Spencer, B., Backman, M., Chakraborty, P., and Hoffman, W. (2014). 3D J-integral capability in Grizzly. Technical Report INL/EXT-14-33257, Idaho National Laboratory, Idaho Falls, ID.

[12] Spencer, B., Hoffman, W., and Backman, M. (2019a). Modular system for probabilistic fracture mechanics analysis of embrittled reactor pressure vessels in the Grizzly code. *Nuclear Engineering and Design*, 341:25–37.

[13] Spencer, B. W., Hoffman, W. M., Biswas, S., and Jain, A. (2020a). Assessment of Grizzly capabilities for reactor pressure vessels and reinforced concrete structures. Technical Report INL/EXT-20-59941, Idaho National Laboratory.

[14] Spencer, B. W., Hoffman, W. M., Biswas, S., Jiang, W., Giorla, A., and Backman, M. A. (2021). Grizzly and BlackBear: Structural component aging simulation codes. *Nuclear Technology*.

[15] Spencer, B. W., Hoffman, W. M., Collins, B. S., and Henderson, S. C. (2020b). Coupling of neutron transport and probabilistic fracture mechanics codes for analysis of embrittled reactor pressure vessels. In *ASME Pressure Vessels and Piping Conference*, pages PVP2020–21680, Virtual, Online. American Society of Mechanical Engineers.

[16] Spencer, B. W., Hoffman, W. M., Schwen, D., and Biswas, S. (2019b). Progress on Grizzly development for reactor pressure vessels and reinforced concrete structures. Technical Report INL/EXT-19-56012, Idaho National Laboratory.

[17] Toptan, A., Porter, N. W., Hales, J. D., Spencer, B. W., Pilch, M., and Williamson, R. L. (2020). Construction of a Code Verification Matrix for Heat Conduction With Finite Element Code Applications. *Journal of Verification, Validation and Uncertainty Quantification*, 5(4):041002.

[18] Williams, P., Dickson, T., Bass, B. R., and Klasky, H. B. (2016). Fracture Analysis of Vessels – Oak Ridge, FAVOR, v16.1, computer code: Theory and implementation of algorithms, methods, and correlations. Technical Report ORNL/LTR-2016/309, Oak Ridge National Laboratory, Oak Ridge, TN.